https://doi.org/10.5194/egusphere-2025-2998
Preprint. Discussion started: 18 July 2025

Assessing extreme total water levels across Europe for large-scale coastal flood analysis

Camila Cotrim[1], Alexandra Toimil[1], Iñigo J. Losada[1], Melisa Menéndez[1], Hector Lobeto[1]

[1]IHCantabria - Instituto de Hidráulica Ambiental de la Universidad de Cantabria, Santander, 30911, Spain

Correspondence to: Alexandra Toimil (toimila@unican.es)

Abstract. Coastal storm-induced flooding threatens millions of people and infrastructures, highlighting the need for comprehensive flood risk assessments. A key component of these assessments is the spatial characterization of total water level (TWL), the primary driver of coastal impacts. We propose a homogeneous methodology for developing large-scale TWL hindcasts to estimate extreme events, considering possible spatial variabilities in marine dynamics. This methodology is applied to the European coastline, integrating downscaled nearshore waves, storm surges, and tides. The resulting hourly time series of the TWL have a spatial resolution of 1 km and covers the period from 1985 to 2021. Spatial variability is considered in foreshore slopes and extreme value detection thresholds, addressing common simplifications in large-scale studies. In addition to a characterization of extreme events based on the relative contributions of TWL components, sensitivity analyses of the wave contribution, wave data resolution, foreshore slopes, and wave setup formulations are conducted. The tide-dominated Atlantic coast is most affected by the wave dataset. The storm surge-dominated Baltic region exhibits the lowest confidence in estimating TWL return levels, partially due to the data and methods used. The Mediterranean Sea, characterized by a mixed environment, is the most sensitive to the inclusion of wave contribution. A classification of TWL extremes revealed that no regions have extreme events dominated by wave setup, while those dominated by tides show the highest return levels.

1 Introduction

The assessment of coastal impacts resulting from extreme coastal flooding events is essential for understanding and mitigating associated potential risks (Neumann et al., 2015). These risks include, among others, damage to coastal infrastructure and the built environment, as well as impacts on the population and ecosystems (Barnard et al., 2019; Rashid et al., 2021; Rasmussen et al., 2022). The total water level (TWL) is the most commonly used indicator in coastal flooding studies. It is frequently used as a forcing variable for flood models aimed at generating maps of flood extent and depth. Accurate coastal flood estimates require that TWL includes a proper spatial characterization of all relevant components (i.e., waves, storm surges, and astronomical tides) (Cabrita et al., 2024; Kirezci et al., 2020; Pugh, 1987). However, estimating extreme TWL at coastal locations becomes increasingly complex as the spatial scale of the study domain increases.

https://doi.org/10.5194/egusphere-2025-2998
Preprint. Discussion started: 18 July 2025

One key challenge lies in the method used to reconstruct the TWL, which requires the selection and characterization of relevant components at appropriate spatial and temporal scales. We consider TWL as a combination of astronomical tide (driven by gravitational forces), storm surge (caused by strong winds and low atmospheric pressures during storms), and a contribution by ocean waves (usually the wave setup, which is an increase of sea level in the surf zone) (Pugh & Woodworth, 2014). Among these, assessing the contribution of waves is particularly critical, as it involves evaluating nearshore wave conditions and the associated wave setup, which depending on the formulation can be influenced by the foreshore slope. A second key challenge concerns the choice of an extreme value analysis (EVA) method. EVA is used to assess the likelihood of extreme events by means of a statistical long-term extreme distribution in order to derive return levels corresponding to specified return periods (Coles, 2001). Each stage in this process introduces uncertainty, from data selection and the formulation used to calculate wave contributions to TWL, to the definition of extreme events (e.g., threshold selection) and the fitting of statistical distributions to estimate return levels (Hinkel et al., 2021; Toimil et al., 2020).

Initial attempts at assessing coastal flood impacts at large scales relied on the DIVA model (Vafeidis et al., 2008), which provided TWL and return level scenarios. More recent efforts have focused on improving the spatial resolution and temporal extent of large-scale TWL hindcasts. For example, TWL has been globally reconstructed from 1993 to 2013 at a 111 km resolution (Vitousek et al., 2017). For the European coastline, TWL from 1979 to 2014 was calculated with a 25 km resolution (Vousdoukas et al., 2016), and from 2010 to 2019 with 2.5 km resolution (Le Gal et al., 2023).

With respect to TWL components, storm surges and astronomical tides are commonly included in flood studies, whereas the wave component is often neglected despite its potential importance along many coasts (Muis et al., 2015, 2016; Paprotny et al., 2016, 2018). At large scales, few studies include wave effects, which may take different forms depending on the processes considered. These include: (1) static wave setup, defined as the superelevation of the coastal water surface due to wave breaking; (2) dynamic wave setup which adds the effect of the infragravity swash to the static wave setup; and (3) wave runup, which further includes the incident swash component (Stockdon et al., 2006). While the estimation of infragravity swash remains uncertain at large scales, incident swash generally does not sustain flooding capable of causing coastal damage (Hinkel et al., 2021). For two-dimensional flood modeling, the wave contribution component is usually represented by the static wave setup (hereafter referred to as wave setup). Several methods exist for estimating wave setup at large scales. The most widely used is the empirical approach proposed by Guza & Thornton (1981), which estimates wave setup as a fraction of the significant wave height (Hs), namely 0.2Hs. However, this method often leads to overestimation of wave setup (Hinkel et al., 2021). More accurate alternatives involve simplified parametrizations. For instance, the semi-empirical formulation by Stockdon et al. (2006) has been adopted globally (Rueda et al., 2017; Vitousek et al., 2017), as well as the Shore Protection Manual method (Kirezci et al., 2020; USACE, 1984). One way these parametrizations improve accuracy is by incorporating nearshore bathymetry, particularly the foreshore slope (Dodet et al., 2019; Gomes da Silva et al., 2020).

https://doi.org/10.5194/egusphere-2025-2998
Preprint. Discussion started: 18 July 2025

A limitation within the use of wave parametrizations lies in accurately characterizing the foreshore slope at large scales. Despite its importance, this parameter remains difficult to quantify, which limits its practical applicability in many coastal assessments. Consequently, some authors applied a constant slope of 1:30 (Kirezci et al., 2020), while others used a wave setup formulation designed for dissipative beaches (Vitousek et al., 2017), that does not require slope data (Stockdon et al., 2006). Alternatively, a method developed by Sunamura (1984) allows for the estimation of spatially and temporally varying foreshore slopes based on wave conditions. Compared with locally observed slopes and globally constant values, this method accounts for morphological feedback, given that evolving beach morphology can influence wave contributions to sea level, as considered in Sunamura's formulation (Melet et al., 2020).

Another limitation in these studies is that offshore wave conditions are often used, despite their coarse resolution and limited suitability for accurately assessing coastal impacts. More precise estimates of coastal flooding require nearshore wave data, which better capture the relevant coastal dynamics, as wave setup is not an offshore process (Dodet et al., 2019). The use of nearshore information is however limited at large geographical scales due to modeling complexity and computational demands, resulting in reduced data availability.

Regarding the second key challenge, the most commonly used approaches for identifying extreme events in EVA include the annual maxima (AM) and the peak-over-threshold (POT) methods (Bezak et al., 2014). Sensitivity analyses in various studies suggest that no single method is optimal for all cases. On the one hand, the AM selects at least one value per year (Haigh et al., 2014a; Paprotny et al., 2016), being most appropriate when a time series longer than 30 years is available. To address the limited sample provided by AM, Vitousek et al. (2017) adjusted the selection of events to the 3-largest events per year. Notably, large-scale studies applying traditional AM to identify a single event per year are mostly centered in storm surge events (Haigh et al., 2014a; Muis et al., 2016; Paprotny et al., 2016). On the other hand, the POT method better exploits the available data by considering that extreme events are independent readings that represent a certain single event (Soomere et al., 2018). Rather than analyzing the temporal distribution of events, POT bases its selection on the magnitude of the events which is directly related to the threshold. Depending on the chosen threshold, larger sample sizes of extremes are obtained than with AM (Kirezci et al., 2020; Le Gal et al., 2023). However, threshold selection is not straightforward. It must be high enough to exclude non-extreme events but low enough to ensure a sufficiently large sample for statistical analysis (Harley, 2017). In addition, the selected maxima peaks must represent independent extreme events, so a minimum span must be considered between two consecutive peaks. A stable threshold based on objective criteria, rather than arbitrary decisions, ensures consistency and more reliable results (Arns et al., 2013). Previous studies have tested different percentiles as the threshold and the 98th percentile (P98) of the TWL time series was used globally (Kirezci et al., 2020) while the 97th percentile (P97) was adopted for the European coast (Le Gal et al., 2023). We note that the selection of a percentile is dependent on the length of the available time series and time resolution, among others. Alternatively, a fixed TWL value can be used, although not suitable for large-scale studies where extreme magnitudes vary widely. To address spatial variability, a threshold corresponding to an average number of independent events per year across the European coastline has also been adopted (Vousdoukas et al., 2016).

https://doi.org/10.5194/egusphere-2025-2998
Preprint. Discussion started: 18 July 2025

The selection of distribution types for estimating return levels also carries important implications that need to be carefully evaluated. For example, two-parameter distributions, such as the Gumbel distribution for AM (Paprotny et al., 2016) or the exponential distribution for POT, simplify the process and are advantageous at large scales due to reduced degrees of freedom and restricted value ranges. However, the three-parameter distributions such as the GEV for AM (Vitousek et al., 2017) and the Generalized Pareto Distribution (GPD) for POT (Kirezci et al., 2020), may yield more robust and stable results (Bezak et al., 2014). Ultimately, the choice depends on regional and data characteristics. Nevertheless, the key features of an EVA application go beyond the method adopted to sample extreme events or the statistical model used to fit the data. Depending on the regional climatic characteristics, data available, and the variables considered (e.g., individual sources, combined drivers, and outputs of coastal hazards), the most suitable approach may vary (Coles, 2001).

Accordingly, in this work, we address the above challenges by proposing a methodology for reconstructing large-scale TWL hindcasts and estimating extreme events. Basing on the hypothesis that a standardized strategy to estimate extreme TWL can effectively capture the diverse conditions governing coastal dynamics across large scales, the objective of this study was to create a homogeneous methodology which considers possible heterogenous marine climate characteristics relevant in coastal storms. We apply our method to the European coastline, producing hourly TWL time series at 1 km resolution spanning from 1985 to 2021. This represents the longest and highest spatial resolution TWL time series for Europe to date, incorporating nearshore wave information. Our TWL formulation includes wave setup, storm surges, and astronomical tides. The wave setup is computed semi-empirically using spatially and temporally varying foreshore slopes. Extreme events are identified using the POT method with a spatially variable threshold, and return levels are estimated with an exponential fit. To demonstrate the robustness of our approach, we conduct a series of sensitivity analyses of the effect different wave component options and POT thresholds have on the assessment of extreme events. For those, return levels extracted from EVA and flooded area derived from a static flood model are used as indicators of the effects certain decisions taken during the extreme TWL estimation process might have on coastal flooding.

2 Data and Methods

The methodology developed to estimate extreme TWL at the large-scale is presented in Fig. 1. We reconstructed a TWL hindcast on an hourly basis by linearly summing time series of wave setup, storm surges, and astronomical tides. The wave setup was estimated with a semi-empirical formulation (Stockdon et al., 2006) considering spatially and temporally variable foreshore slopes (Sunamura, 1984). To identify extreme events in the TWL hindcast, we applied the POT method, using a spatially variable threshold. The selected extreme events were fitted to an exponential function to estimate return levels. Different steps of the methodology were evaluated and validated through sensitivity analyses focusing on: (1) wave contribution; (2) components of wave setup; and (3) the POT threshold.

https://doi.org/10.5194/egusphere-2025-2998
Preprint. Discussion started: 18 July 2025

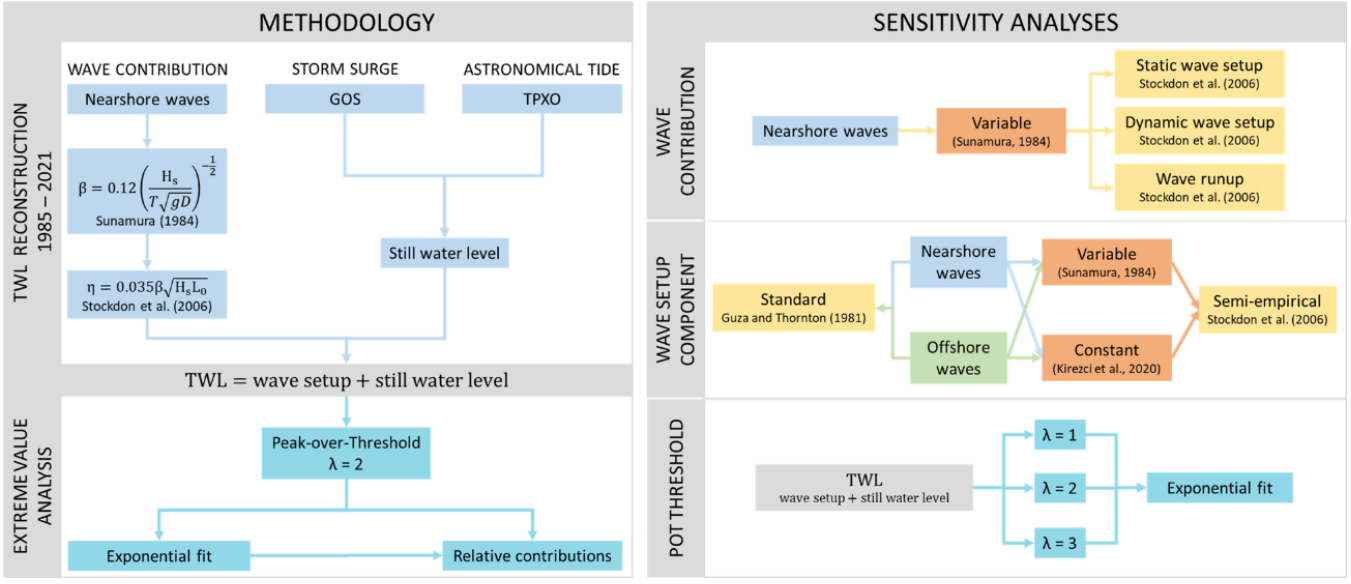

Figure 1: Methodology applied in the present study for TWL hindcast reconstruction and extreme value analysis (left). Sensitivity analyses applied to the wave contribution, wave setup components, and POT threshold (right).

2.1 Study Area

The study area comprises the European coastline. Prior to reconstructing the TWL hindcast, coastal target points (CTP) were defined along the European coast. These points were used for downscaling wave conditions and reconstructing the TWL, with the objective of creating a continuous line of equally spaced points as close to the coast as possible. Due to the lack of high-resolution homogeneous bathymetry data at this scale, the CTPs were selected based on their relative depth (h/L), where *h* represents the water depth and L the corresponding wavelength of the wave peak period with an exceedance probability of 0.1. In total, 51010 CTP with relative depth of approximately 0.1 were chosen, with an interval of 1 km between them and as close as possible to the coast.

2.2 Climate-related Datasets

The still water level includes the mean sea level, astronomical tide, and storm surge. Here, the local mean sea level is used as benchmark. The hourly time series of the astronomical tide and storm surge were reconstructed from the tidal constituents of the TPXO9 model (Egbert & Erofeeva, 2002) and from a European regional storm surge hindcast developed using the ROMs model (Shchepetkin & McWilliams, 2005), respectively. The astronomical tide provides data in coastal areas at a spatial resolution of 1/30° (approximately 3.5 km), whilst the European storm surge hindcast used provides storm surge information along the European coast at 5-11 km spatial resolution. The offshore waves were obtained from a European regional hindcast developed with the WaveWatchIII numerical model (Tolman, 2009). This provides wave outputs along the

https://doi.org/10.5194/egusphere-2025-2998
Preprint. Discussion started: 18 July 2025

European coastline at a spatial resolution of 1/8° (10-15 km). The nearshore wave dataset was developed based on the DOW approach (Camus et al., 2013), which combines numerical wave simulations using the SWAN model with advanced statistical techniques in order to reach 1 km spatial resolution throughout the European coastline. Atmospheric forcings from the ERA5 reanalysis (Hersbach et al., 2020) were used to generate these datasets consistently. A more detailed description of the models and their configuration used, as well as an assessment of the data quality in coastal areas by comparison against coastal buoys and tide gauge records is provided in the Sea level and wave datasets section of the Supplementary Material.

At each CTP, hourly time series were obtained for the astronomical tide, storm surge, offshore wave conditions and nearshore wave conditions. As the offshore wave hindcast, storm surge hindcast, and TPXO databases do not share the same spatial resolution as the nearshore wave dataset, the data from the nearest grid point was assigned to each CTP for those variables.

2.3 Total Water Level

The TWL time series from 1985 to 2021 on an hourly basis at each CTP by linearly adding the time series of astronomical tide, storm surge, and wave setup (1).

$$\mathrm{TWL} = \text{wave setup} + \mathrm{SS} + \mathrm{AT} \tag{1}$$

where SS is the storm surge and AT the astronomical tide.

Wave setup was used to represent the wave contribution to TWL. Using nearshore wave conditions, it was calculated with the semi-empirical formulation, (2) and (3) (Stockdon et al., 2006) with a variable intertidal slope, (4) (Sunamura, 1984).

$$\eta = 0.035\beta\sqrt{H_s L_0} \tag{2}$$

$$L_0 = \frac{gT^2}{2\pi} \tag{3}$$

where β is the foreshore slope of the beach, between the low and high tide limits, H_s is the significant wave height, L_0 is the deep-water wavelength, and T is the wave period.

$$\beta = 0.12\left(\frac{H_s}{T\sqrt{gD}}\right)^{-\frac{1}{2}} \tag{4}$$

where g is gravitational acceleration and D is the mean sediment grain size, set at 250 µm, representative of fine to medium grain size and following Rueda et al. (2017). The calculated foreshore slope time series for each CTP was capped at 0.20 and normalized to ensure a mean close to 0.04, reflecting the global median beach slopes reported locally (Barboza & Defeo, 2015). The approach used to apply the approximation for the foreshore slope followed Melet et al. (2020).

Upon the TWL reconstruction, the stationarity of the time series was verified in each CTP and a validation of the hindcast was performed by identifying historical coastal storms observed in the literature and comparing to the values estimated here. In total, 36 events were validated for different events and across distinct areas of the European coastline. A summary of the references and locations validated is presented in the Supplementary Material. The validation was performed against still

https://doi.org/10.5194/egusphere-2025-2998
Preprint. Discussion started: 18 July 2025

water level, static wave setup-based TWL, dynamic wave setup-based TWL, and wave-runup-based TWL, following Stockdon et al. (2006).

2.4 Extreme Value Analysis

The POT method was used to identify extreme events in the TWL hindcast. At each CTP, we selected a threshold that resulted in an average of two events per year, with a minimum interval of 72 hours between events. Next, we estimated the TWL return values (i.e., TWL values associated with return periods) by fitting the extreme sample to an exponential model. To refine the methodology, we conducted several tests regarding the extreme event selection method, the threshold applied and the distribution fits. Preliminary tests applied were carried out on a set of points selected using clustering methods (Camus et al., 2011), as detailed in the Supplementary Material (Fig. S4). We compared the results of return levels and confidence intervals obtained from AM method using GEV and Gumbel distributions, and from the POT method using both exponential and GPD fits (Supplementary Fig. S5), as well as different thresholds options tested in POT (Supplementary Fig. S6). The initial thresholds tested included the five lowest annual maxima at each CTP. A stability check of the resulting parameters was assessed through a residual life plot (Coles, 2001; Liu et al., 2023) (Supplementary Fig. S7) and concluded that the optimal average amount of events per year (λ) was two. At the European scale, we validated the resulting fit using various tests, including the Anderson-Darling test and an assessment of the significance of the shape parameter (Supplementary Fig. S8 and Supplementary Fig. S9).

2.5 Relative Contributions of TWL components

To better understand the dominant conditions at each CTP, the relative contributions of each TWL component were computed (astronomical tide, storm surge, and wave setup). The contribution of each component was calculated by extracting its value from its respective time series at the corresponding time step and determining its proportion relative to the TWL. For mean conditions, we calculated this for each time step within the entire time series and then calculated the mean contribution for each component. For the extreme conditions, relative contributions of each TWL component were calculated for each peak identified by the POT.

2.6 Sensitivity Analyses

Figure 1 also presents the three sensitivity analyses performed. The first two analyses refer to the inclusion of waves in a TWL study, while the third analysis examines the adopted threshold as part of EVA. Within these analyses, the EVA method (POT followed by exponential fit) was adopted in all cases. Two indicators were used to determine how sensitive results are to the different options tested in each analysis. On the one hand, the 100-yr TWL resulting from an exponential fit was analyzed. The variability of results was studied to determine the relative influence each option has on the outcome. On the other hand, the corresponding 100-yr TWL flooded area (FA) resulting from a static flood model applied to the European

https://doi.org/10.5194/egusphere-2025-2998
Preprint. Discussion started: 18 July 2025

floodplain was evaluated. The floodplain was defined as the terrain below 15 m in elevation and hydraulically connected to the sea, based on the 25 m resolution Copernicus EU-DEM (Copernicus, 2019).

2.6.1 Sensitivity analysis: wave contribution

As part of the validation of the TWL reconstruction, different options were tested in terms of the characterization of the wave contribution. Following the equations by Stockdon et al. (2006) with a variable intertidal slope, (4) (Sunamura, 1984) we tested: (1) static wave setup, following equation (2); (2) dynamic wave setup, as in equations (5) and (6); and (3) wave runup, equation (7). After each wave contribution was computed, the corresponding TWL was reconstructed by adding the storm surge and astronomical tide time series. The same resulting TWL variants used in this analysis, were the ones adopted in the TWL reconstruction validation.

$$S_{IG} = 0.06\sqrt{\mathrm{H_s L_0}} \tag{5}$$

$$\eta_{dyn} = \eta + S_{IG} \tag{6}$$

$$R_2 = 1.1\left(\eta + \frac{\sqrt{H_s L_0 (0.563\beta + 0.004)}}{2}\right) \tag{7}$$

2.6.2 Sensitivity analysis: wave setup components

Three elements were tested in the wave setup analysis: (1) the wave dataset (downscaled nearshore wave conditions and large-scale wave conditions, hereafter referred to as offshore wave conditions); (2) the foreshore slope approximation (variable and constant); and (3) the wave setup formulation (semi-empirical and standard). The combinations of these elements resulted in six TWL reconstruction approaches. While approach A represents the methodology developed in the present study, the remaining approaches were only used in this sensitivity analysis.

First, we calculated wave setup with the same formulation (2) but applying offshore wave conditions instead of nearshore downscaled conditions. Then, we applied the wave setup formulation by Guza & Thornton (1981) to both offshore and nearshore wave conditions (8).

$$\eta = 0.2\mathrm{H_s} \tag{8}$$

For the comparison of foreshore slope approximations, we applied the variable slope approximation (Sunamura, 1984) to offshore wave conditions and also adopted a constant foreshore slope of 0.03 (Kirezci et al., 2020). Both foreshore slope options were used in conjunction with the semi-empirical wave setup formulation shown in equation (2) (Stockdon et al., 2006) and with both wave datasets. In total, six approaches were tested, as shown in Table 1. The same EVA method (POT with a threshold of λ=2 fitted to an exponential fit) was applied to all approaches to obtain the 100-yr return levels.

https://doi.org/10.5194/egusphere-2025-2998
Preprint. Discussion started: 18 July 2025

Table 1: Approaches used to reconstruct TWL in the sensitivity analysis of wave setup components, showing their respective combinations of wave datasets, foreshore slope approximations, and wave setup formulations adopted.

Approach	Dataset	Foreshore slope	Wave setup
A	Nearshore	Sunamura (1984)	Stockdon et al. (2006)
B	Nearshore	Kirezci et al. (2020)	Stockdon et al. (2006)
C	Nearshore		Guza and Thornton (1981)
D	Offshore	Sunamura (1984)	Stockdon et al. (2006)
E	Offshore	Kirezci et al. (2020)	Stockdon et al. (2006)
F	Offshore		Guza and Thornton (1981)

2.6.3 Sensitivity analysis: POT threshold

Since the POT method is sensitive to the chosen threshold, which can introduce subjectivity and affect the results, a sensitivity analysis is needed to assess how robust and consistent the estimates are. Although the threshold selected in this study corresponds to a variable value corresponding to an average of 2 extremes events samples per year (λ=2) in each CTP, other options were tested. The variability in the extreme TWL results was also analyzed for occurrence rates of λ=1 and λ=3. The exponential distribution was fitted to the three resulting thresholds to obtain the 100-yr return levels. Outcomes were examined through the variability of results, Anderson-Darling tests, and the uncertainty represented by the 95th confidence intervals of 100-yr TWL.

3 Results

3.1 Wave and sea level datasets processing and total water level computation

Figure 2 presents the 2021 hindcast of all variables used in this study for four coastal target points (CTP) in which we reconstructed the TWL hindcast. The CTPs used as examples throughout this study were selected from a list of test points. The locations of the test points are presented in the Supplementary Fig. S4. Point 1 is located on the Atlantic coast of France, point 2 in Estonia in the Baltic Sea, point 3 in Greece in the Mediterranean Sea, and point 4 in Norway (Fig. 2g). These points represent the centroids of the four most distinct clusters obtained from a K-means clustering applied to the relative contributions of the TWL components. Offshore wave conditions (Fig. 2a) were downscaled to the coast (hereinafter, nearshore wave conditions; see Fig. 2b), from which wave setup (Fig. 2c) was calculated to represent the wave component. The nearshore wave dataset accounts for the presence of ice at higher latitudes. Storm surge (Fig. 2d) and astronomical tide

https://doi.org/10.5194/egusphere-2025-2998
Preprint. Discussion started: 18 July 2025

data from TPXO (Fig. 2e) were then added to the wave setup hindcast to obtain the TWL (Fig. 2f) time series. As a consequence, the variability of the TWL reflects the heterogeneity of the spatial distribution of its three components. The distinction between offshore and nearshore wave conditions is evident, particularly at points 3 and 4 where notable differences are observed. The results highlight that while the TWL time series of points 1 and 5 are primarily influenced by tides, point 2 appears to be dominated by storm surge. However, although point 4 shows smaller oscillations, higher wave setup values raise its TWL time series, unlike point 1, where the series remains centered around 0 m.

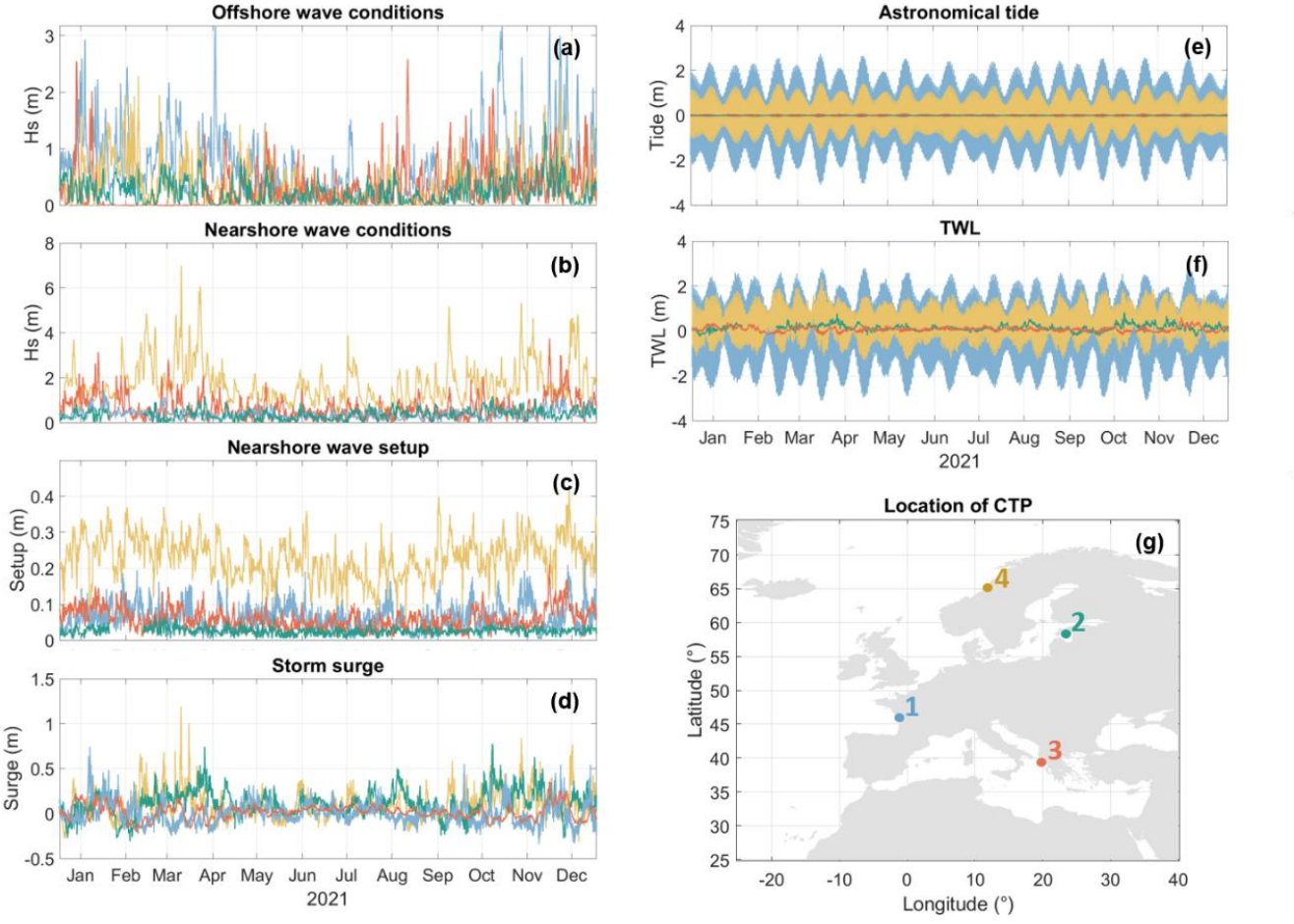

Figure 2: Hindcast time series referred to 2021 for the following variables: offshore significant wave height (a), nearshore significant wave height (b), nearshore wave setup (c), storm surge (d), astronomical tide (e), and TWL (f). Location of the CTPs used as examples (g). Time series are represented in the same colors as its corresponding CTP.

3.2 Validation of TWL reconstruction

Figure 3 presents the validation of the TWL hindcast reconstruction. The validation was performed by comparing our estimated values against previously observed historical storms across the study area, based on previous studies. For more

https://doi.org/10.5194/egusphere-2025-2998
Preprint. Discussion started: 18 July 2025

details on the references used in the validation of the TWL, please refer to the Supplementary Material (Table S2). In total, five TWL approaches were tested: still water level (astronomical tide and storm surge) (Fig. 3a), TWL with static wave setup (Fig. 3b), TWL with dynamic wave setup (Fig. 3c), TWL with wave runup (Fig. 3d), and TWL considering the most similar result in each point, referred to as the best approach (Fig. 3e). The latter presents the best performance in estimating historical extreme TWL events with 98.1% of the TWL variability being captured, an RMSE of 0.173 m, and a bias of 0.023 m. However, given the large-scale aspect of this study, applying a heterogeneous method such as this is not feasible due to the different climatic conditions one might encounter and the fact that not all CTPs have been validated in order to identify which would be the best approach in each case. Within the four remaining options available for a homogeneous TWL reconstruction approach at the large-scale, the TWL based on static wave setup shows the best performance with 87.9% of the TWL variability being captured, an RMSE of 0.438 m indicating an average error of 7.5%, and a bias of -0.151 m. Meanwhile, TWL based on still water level leads to a greater level of underestimation and the remaining two approaches, an even greater level of overestimation. These results highlight the importance that other aspects might have on the resulting TWL and, consequently, coastal flooding. Notably, the cases in which static wave setup underestimates TWL the most are located along the Atlantic coast, such as Santander (Spain), Brouage (France), and the Ebel Estuary (Germany). This could be an indication that these regions are sensitive to infragravity waves, provided that dynamic wave setup offers a more accurate estimate of TWL.

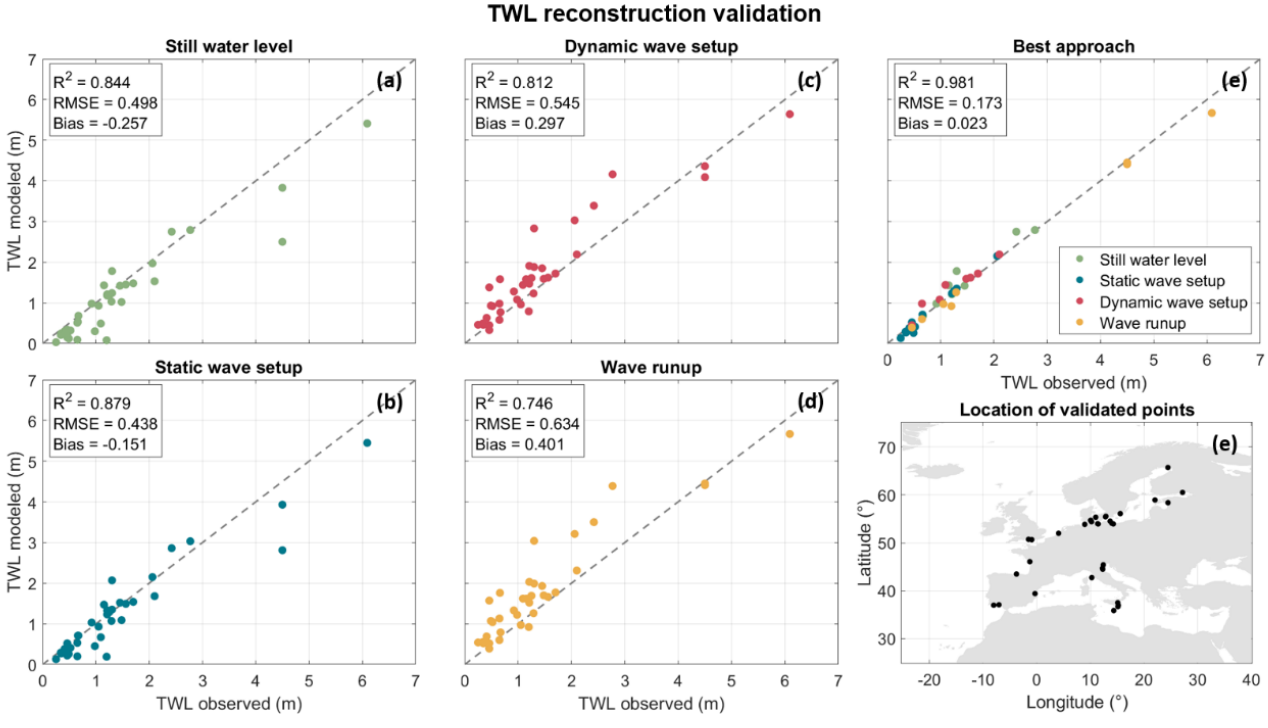

Figure 3: TWL reconstruction validation based on TWL with still water level (a), static wave setup (b), dynamic wave setup (c), wave runup (d), and based on the best approach when comparing historical coastal storms observed in different points across the study area (e), according to previous studies.

https://doi.org/10.5194/egusphere-2025-2998
Preprint. Discussion started: 18 July 2025

3.3 Extreme value analysis of the total water level

Figure 4 shows the TWL threshold used in the POT method to select the extreme events (Fig. 4a) as well as the corresponding TWL percentiles associated with these thresholds for each CTP (Fig. 4b–c). The results emphasize the importance of considering the spatial variability of thresholds as neither the TWL thresholds nor the corresponding percentiles are uniform across the study area. When adopting λ=2, the TWL threshold ranges from 0.3 m in the Messina Strait (Italy) to 7.2 m in the Bristol Channel (Great Britain), while corresponding percentiles range from P31.6 near the Lofoten Islands (Norway) to P99.9 in the Wash (Great Britain). Approximately 85.5% of the coastline is characterized by percentiles above the P99. Regions such as northern Norway and the Baltic Sea exhibit lower percentile equivalence, between P31.6 and P90. This may be attributed to the presence of ice, which is considered in this study. When providing shoreline protection by acting as a physical barrier against high water levels, this variable lowers the baseline conditions, allowing for even small disturbances to cause impacts (Wang & Bernier, 2023). When applying a constant percentile threshold across the study area, λ varies from 12.1 to 68.3 for P90 and 1.4 to 14.5 for P99.5. This suggests that using a constant threshold would lead to an excessive number of events in regions such as the Dutch coast and the Irish Sea, for example. Whereas in others regions, such as the Baltic Sea, the sample size would be insufficient, resulting in unstable results of EVA and return levels of TWL. The spatial distributions of λ using P90 and P99.5 constant thresholds are provided in Supplementary Fig. S10.

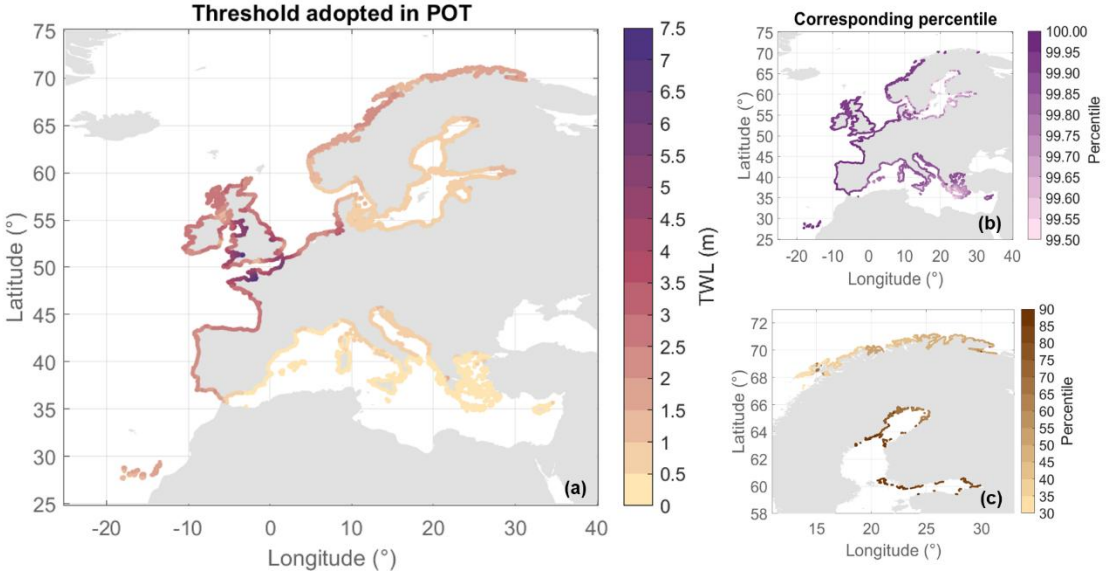

Figure 4: TWL threshold adopted in each CTP for the POT analysis (a). TWL percentile that corresponds to the threshold adopted in each point, highlighting points where the associated percentile is above P99.5 (b) and lower than P90 (c).

https://doi.org/10.5194/egusphere-2025-2998
Preprint. Discussion started: 18 July 2025

Figure 5 provides the spatial distribution of the 100-yr TWL for the coast of Europe and the associated 95th confidence interval values (Fig. 5b) at each CTP. This result is shown in percentage relative to the return level itself to facilitate the comparison of the results between different regions. For example, the 100-yr TWL in France is 3.5 ± 0.12 m, or 0.3% (Fig. 5c). While in Estonia it is 1.6 ± 0.17 m, or 10.8% (Fig. 5d) and in Greece, it is 0.7 ± 0.07 m, or 9.8% (Fig. 5e). Higher confidence interval values indicate a broader confidence band and, consequently, greater uncertainty in the distribution fit. With TWL values reaching up to 8.5 m in the Bristol Channel, the highest 100-yr TWL values are observed around the British Isles and along the English Channel. This region also shows the narrowest confidence intervals, with the confidence band fluctuating by less than 4% for the 100-yr TWL. This may be linked to the dominant tidal regime in this area, which due to its high amplitude modulates both mean and extreme conditions. The Mediterranean Sea shows the lowest 100-yr TWLs, with values ranging from 0.49 m in the Messina Strait to 2 m in the Adriatic Sea. In this region, the 95th confidence interval increases from approximately 6.5% in the Gibraltar Strait to 11% in Greece. In the Baltic Sea, 100-yr TWL range from 0.91 m south of Stockholm to 2.52 m in St. Petersburg, increasing towards the regions of the inner gulfs. Additionally, this region displays the widest confidence intervals, ranging from 9% to 12% for the 100-yr TWL. Overall, these results suggest that return level estimates are more reliable in areas where TWL is dominated by the astronomical tide, such as the Bay of Biscay, where confidence intervals range from 2% to 5%. Similar behavior, albeit with slightly lower values, is observed for the 50-yr TWL (see Supplementary Fig. S11).

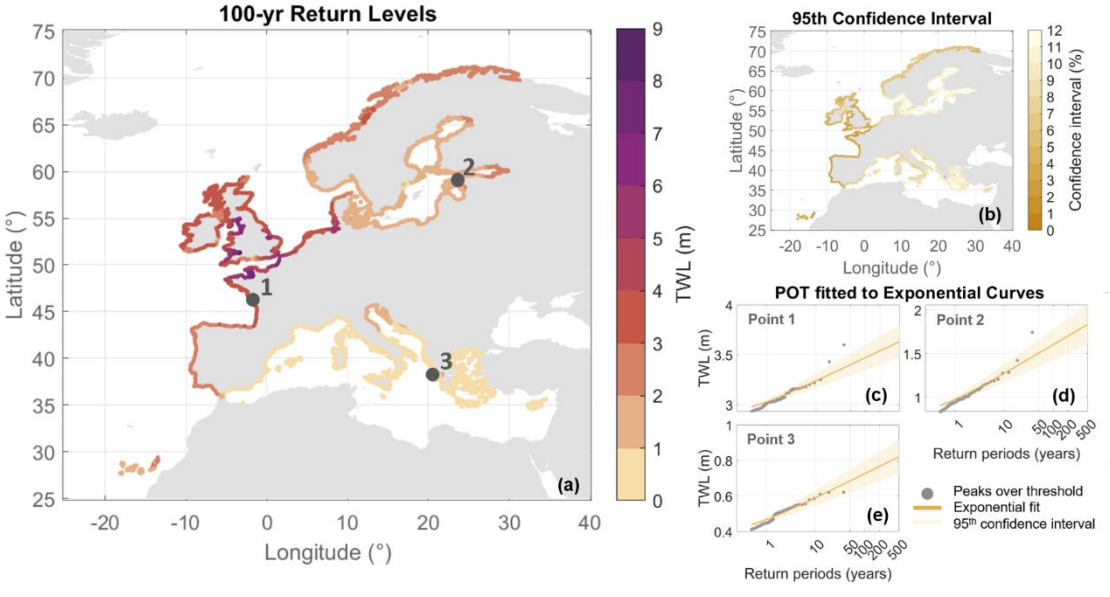

Figure 5: Spatial distribution of the 100-yr return period TWL resulting from POT with an exponential fit (a). Spatial distribution of the 95th confidence interval relative to the 100-yr TWL event, in percentage (b). Examples of individual CTP with the exponential fits applied to the POT samples to extract return levels of TWL (c, d, e).

https://doi.org/10.5194/egusphere-2025-2998
Preprint. Discussion started: 18 July 2025

3.4 Relative contributions of mean and extreme total water levels

Figure 6 displays the average storm conditions based on the relative contribution of TWL components at peak moment. Examples are shown for three points: point 1 on the Atlantic coast of France (Fig. 6a), point 2 in Estonia in the Baltic Sea (Fig. 6b), and point 3 in Greece in the Mediterranean Sea (Fig. 6c). The shape of the average storm at each point reflects the dominant TWL component during storms. We observe distinct behaviors: point 1 is tide-dominated, point 2 is storm surge-dominated, and point 3 reflects mixed-storm conditions. While point 1 shows semi-diurnal tidal oscillations, point 2 exhibits a single TWL peak, characteristic of a typical storm surge event. Point 3 shows a similar pattern to point 2, but also includes tidal noise throughout the average event. The spatial distribution of TWL component contributions is presented in Fig. 6d–f. Although diverse, it is possible to observe patterns across the study area and the larger European regions previously identified in the study: Atlantic coast, Baltic Sea, and Mediterranean Sea. Figure 6 also presents the dispersion of relative contributions of TWL components, aggregated per European basin. These help with the graphical representation of the uncertainty surrounding the different patterns observed and the characterization of three macro-regions (Fig. 6g–i).

First, the dominance of the astronomical tide along the Atlantic coast is evident and modulates storms regardless of their origin, although at different levels depending on the basin. Tidal contributions along the most exposed Atlantic coast can reach 100%, especially along the Atlantic Iberia and Bay of Biscay. The more northern basins tend to present less dominance of the astronomical tide and more presence of storm surge and wave setup. Notably, the North Sea is the most balanced basin in this region in terms of the contributions of the three components. This is likely due to its shallow waters and extensive continental platform which enhance the action of storm surge. Second, the highest storm surge contributions found in the Baltic Sea also reach 100%. Storm surge tends to be higher in the Baltic Sea due to its wider continental platform. The transition role of the Kattegat Bay is reflected in the higher contribution of astronomical tide as opposed to the remaining two basins. Third, although the highest wave setup contributions are in the Mediterranean Sea, this region also experiences storm surge contributions above 50%. Within this region, the Adriatic Sea shows the highest contribution of storm surge likely because of its shallow water enabling the propagation of storm surges as well as the its lower level of exposure to incoming waves. Meanwhile, the Ionian Sea presents the highest contributions of wave setup, likely because of its exposure levels and lower astronomical tide when compared to the Central Mediterranean basin.

The results show that even in parts of the Baltic and Mediterranean Seas the tide reaches a contribution of more than 20%. These results reinforce the need to account for all three TWL components. Wave setup is particularly relevant under average conditions, especially in semi-enclosed seas (see Supplementary Material). Astronomical tide becomes crucial during the most extreme conditions, even in microtidal areas. Storm surges, often the primary source of extreme TWL, tend to sustain elevated water levels for extended periods. Neglecting any one of these components may lead to an underestimating TWL, particularly if a storm coincides with a spring high tide, thereby increasing coastal risk.

https://doi.org/10.5194/egusphere-2025-2998
Preprint. Discussion started: 18 July 2025

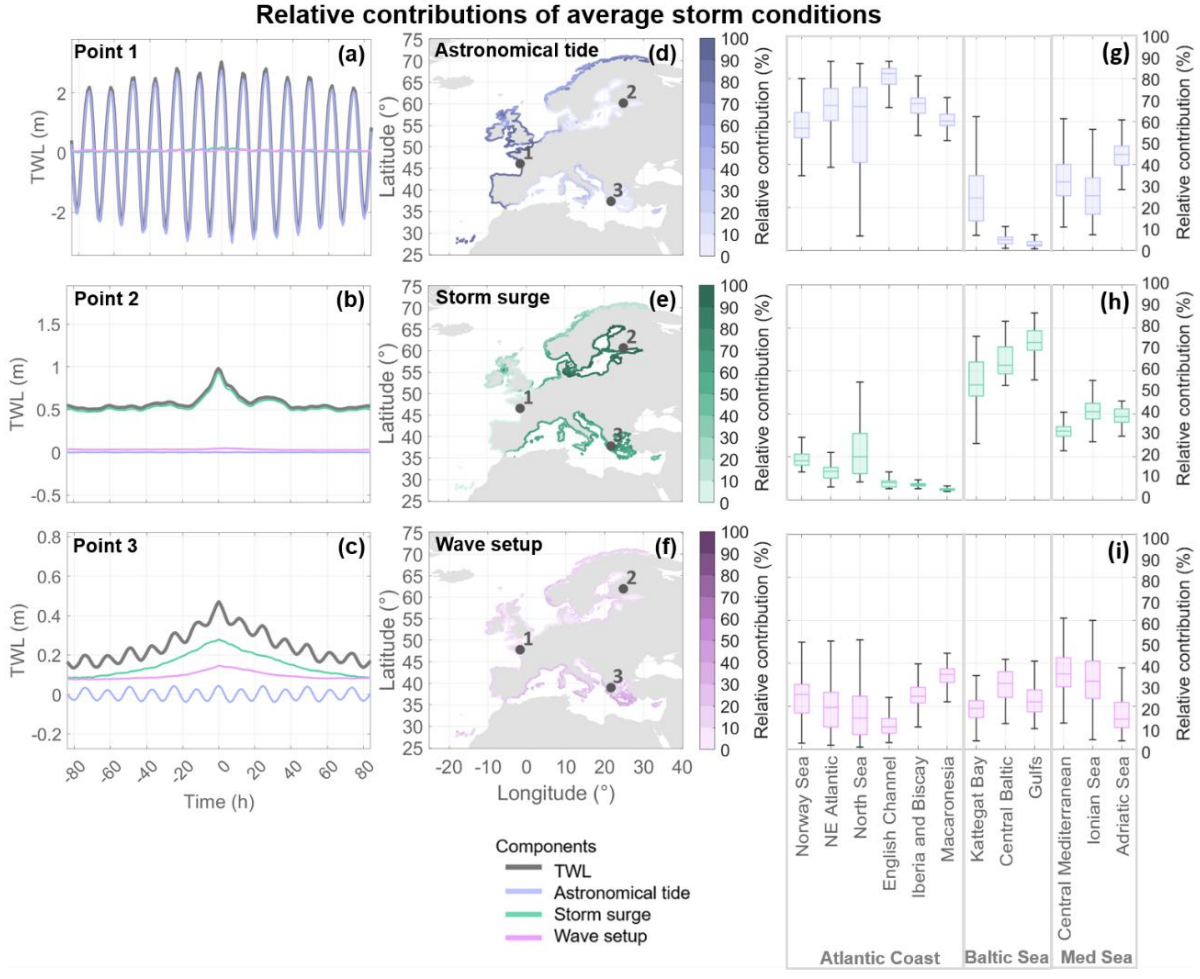

Figure 6: Examples of individual CTP with average storm conditions per TWL component (a, b, c). Spatial distribution of mean relative contributions of astronomical tide (d), storm surge (e), and wave setup (f) under extreme conditions. Dispersion of relative contributions of TWL components per European basin, grouped per European region (g, h, i).

3.5 Sensitivity analysis: wave contribution component

Figure 7a presents the variability of 100-yr TWL given the different options of wave contribution component: static wave setup, dynamic wave setup, and wave runup. The highest variabilities are observed in the Mediterranean Sea which could be an indication of higher contributions of waves to TWL compared to the remaining two components or a response to low ranges of TWL, indicating that even a slight change in the wave contribution is noticed in the estimation of TWL extremes. Meanwhile, the lowest variabilities are found in the Baltic Sea, probably a response to its limited exposure to incoming waves.

https://doi.org/10.5194/egusphere-2025-2998
Preprint. Discussion started: 18 July 2025

Figure 7b presents the FA per European basin, relative to their respective floodplain area, under the 100-yr TWL when adopting different wave contribution components. Overall, the highest increase in the FA happens when changing from a static wave setup based-TWL to a dynamic wave setup based-approach. The basins most affected include Central Mediterranean and Iberia and Biscay. The former is located in a region typically known for coastal wave storms (Lobeto et al., 2024). The latter indicates to be a region sensitive to infragravity waves, which had been observed in the TWL reconstruction validation as well. Meanwhile, the least affected basins are Kattegat Bay and the Gulfs, both located in the Baltic Sea. Besides presenting low values of TWL, these basins are also amongst the steepest floodplains. However, when looking at the macro EU regions, the most affected one is the Mediterranean Sea, followed by the Atlantic coast and the Baltic Sea. These results indicate a possible spatial variability of the wave contribution to TWL. Finally, the European FA under static wave setup is 36.82%, with dynamic wave setup it is 40.40%, and with wave runup it increases to 41.23%. These results show that while the large-scale results do not change much, it is important to zoom in to smaller regions and basins to identify areas in which such decisions might affect the most.

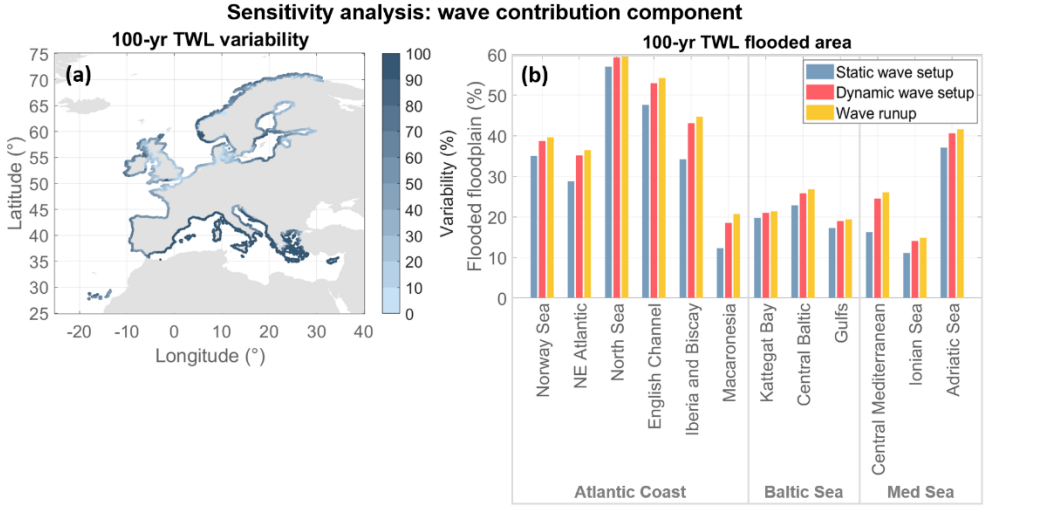

Figure 7: Sensitivity analysis of the wave contribution considered in the TWL reconstruction: static wave setup vs dynamic wave setup vs wave runup. (a) 100-yr TWL variability found in the results. (b) Results of flooded area proportional to the floodplain in each European basin considering the 100-yr TWL.

3.6 Sensitivity analysis: wave setup components

Figure 8 presents the sensitivity analysis of the different TWL approaches tested, using the 100-yr TWL as the indicator. Figure 8a compares this indicator under offshore versus nearshore wave conditions. Positive values indicate that offshore TWL is higher than the nearshore TWL, and negative values indicate the opposite. The results highlight the spatial variability of the TWL outcomes. Generally, offshore data results in lower TWL along the Atlantic coast and higher TWL in the Baltic and Mediterranean Seas compared to nearshore data. This suggests a greater degree of wave transformation on the

https://doi.org/10.5194/egusphere-2025-2998
Preprint. Discussion started: 18 July 2025

Atlantic coast than in the semi-enclosed seas. These discrepancies can be explained by the geometry and exposure of the different regions. First, the steeper bathymetry of the Atlantic coast enhances wave shoaling processes, leading to higher waves as they approach the shore. In contrast, the shallower waters and gentler slopes in the Mediterranean and Baltic Seas could result in greater wave energy dissipation, as waves encounter the seabed earlier and lose energy more quickly. Although not accounted for in this study, non-linear processes involved in wave transformation, such as refraction and wave-breaking mechanisms, could be the reason behind such differences as wave transformation processes affect TWL mainly in areas with steep beach slopes and complex offshore bathymetry (Serafin et al., 2019). Second, the Atlantic coast has a larger fetch, allowing for the development of higher waves, and is more exposed to coastal winds, which amplifies wave energy. Conversely, the Mediterranean Sea has a smaller fetch, producing more localized and less energetic waves. These factors also result in greater discrepancies in wave conditions within the semi-enclosed seas compared to the Atlantic coast, where offshore and nearshore wave conditions are more similar.

Figure 8b identifies the most influential wave component when comparing different TWL modeling approaches. Using the 100-yr TWL as an indicator, 29% of CTPs are most sensitive to dataset selection, while 0.1% are most influenced by the foreshore slope approximation and 70.1% are most influenced by the wave setup method. Dataset selection is the dominant factor along the Atlantic coast. In contrast, the wave setup formulation becomes more important in the semi-enclosed Baltic and Mediterranean Seas. These differences arise from the increased need for accurate data when modeling a wider range of wave conditions. This is particularly critical along the Atlantic coast, where the wave climate is highly energetic (Lobeto et al., 2024). On the other hand, the marginal seas, such as the Baltic or the Mediterranean, exhibit lower TWLs making the accuracy of wave setup estimation crucial. Even the smallest errors in this component can lead to significant discrepancies in the TWL predictions, potentially affecting the accuracy of coastal impacts assessments. Additionally, the low influence the foreshore slope approximation may be due to the conservative approach adopted for capping and normalizing the foreshore slopes (Melet et al., 2020).

Figure 8c presents the influence each wave contribution component tested has on the resulting 100-yr TWL FA, averaged per European basin. Across the entire study area, the most influential element is the wave setup formulation with values ranging from 49.3% along the NE Atlantic basin to 84.0% in the Central Baltic Sea. When comparing the dataset and the slope approximation elements, the Baltic Sea presents more influence from the slope approach, with the exception of the Kattegat Bay which could be described as a transition region rather than being part of the Baltic Sea. Moreover, Central Mediterranean also presents higher influence of the slope approximation than the dataset. The difference, however is only 0.2%. The remaining basins across the study area, show the slope approach as the least influential element. When comparing the influences of the dataset and the wave setup formulation, most of the study area present a negative correlation. Along the Atlantic coast and the Baltic Sea, as the influence of the dataset increases, the influence of the wave setup formulation decreases.

https://doi.org/10.5194/egusphere-2025-2998
Preprint. Discussion started: 18 July 2025

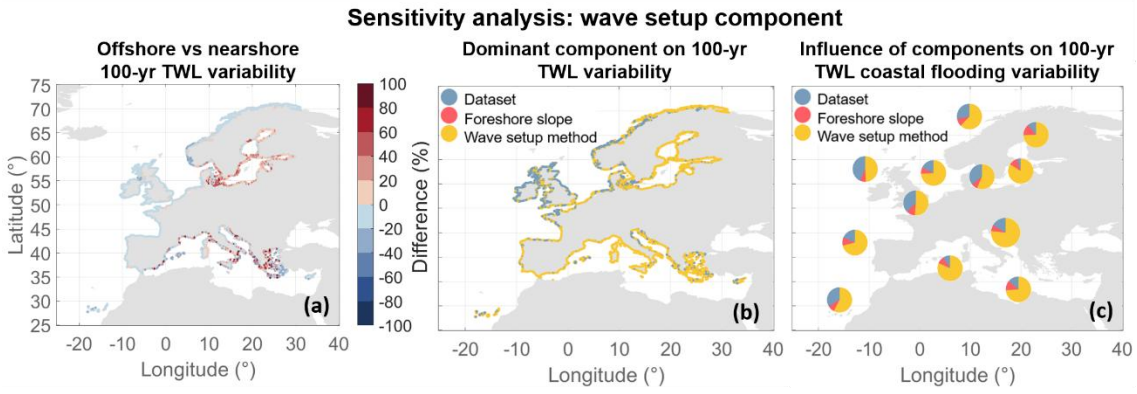

Figure 8: Sensitivity analysis of the wave setup components: data resolution, foreshore slope approximation, and wave setup formulation. (a) Differences in 100-yr TWL when applying offshore instead of nearshore wave conditions. This plot isolates the influence of wave data resolution by comparing TWL approach D against A. (b) Dominant component explaining the 100-yr TWL variability. (c) Influence of wave setup components on the 100-yr flooded area variability averaged per EU basin.

3.7 Sensitivity analysis: POT threshold

Figure 9 presents the sensitivity analysis regarding the POT threshold, comparing EVA results when adopting a variable threshold corresponding to an average of 1 event per year (λ=1), 2 events (λ=2), or 3 events (λ=3). Although the corresponding TWL threshold varies up to 30%, the resulting 100-yr TWL up to 20% (Fig. 9a), and the corresponding 95th confidence interval up to 4%. The highest TWL threshold variabilities occur in the Baltic Sea, whereas the highest 100-yr TWL variabilities occur in the Mediterranean. Meanwhile, the Atlantic coast is the least sensitive to the POT threshold selection. Figure 9b display results of an Anderson-Darling test when adopting the different POT thresholds. A rejected null-hypothesis indicates that the sample does not fit an exponential curve. Out of the 51,010 CTPS, only 121 CTPs indicate that none of the options lead to robust samples. The results shown for λ=1 and λ=2 are similar, with approximately 6.5% of the CTPs not adjusting well to an exponential fit. Meanwhile, λ=3 leads to more than double of the number of CTPs rejecting the null hypothesis (15.3%). Figure 9c–d indicate which threshold tested lead to the highest and lowest uncertainty as represented by the 95th confidence interval of the 100-yr TWL EVA results. Although, λ=1 indicates an overall good fit of the samples in the Anderson-Darling test, this is the threshold leading to the highest uncertainty of return levels. A possible explanation is that λ=1 leads to excessively small sample sizes, leading to instability in the EVA. Meanwhile, although adopting λ=3 yields the lowest uncertainty in most CTPs, the confidence interval difference between λ=2 and λ=3 remains below 1% for the majority of CTPs, indicating minimal impact for 73.3% of the CTPs. For results on the TWL threshold variability, confidence interval variability, and Anderson-Darling test spatial distributions, please refer to the Supplementary Material.

Ultimately, there is no single threshold which solves the different challenges in all 51,010 CTPs. However, given the poorer results from the Anderson-Darling test with λ=3, the higher uncertainties of the estimated return levels provided by λ=1, and

https://doi.org/10.5194/egusphere-2025-2998
Preprint. Discussion started: 18 July 2025

the overall low 100-yr TWL variability across the different methods, λ=2 represents a reasonable balance between accuracy, robustness, and sample size to be used in EVA.

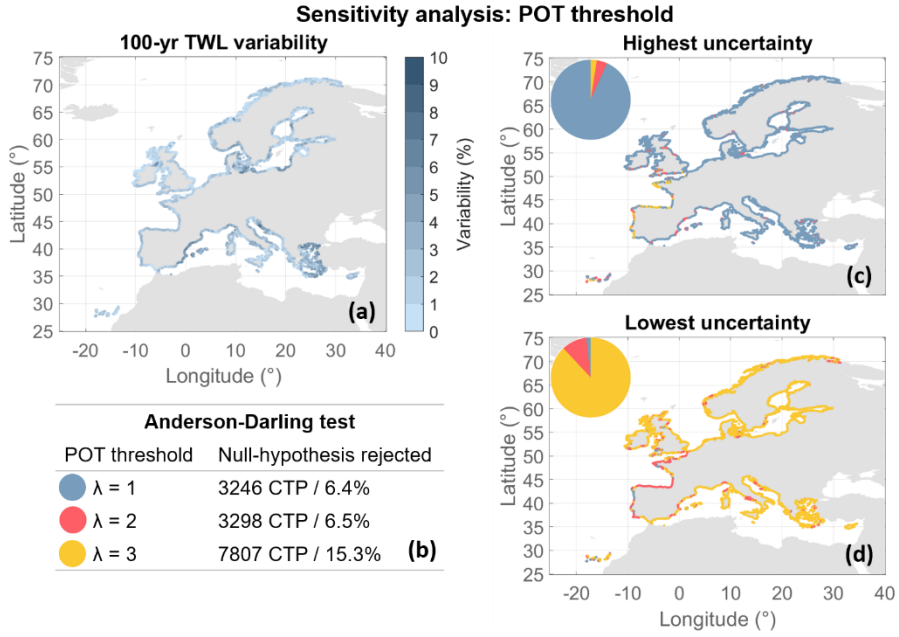

Figure 9: Sensitivity analysis of the POT threshold selected. Variable thresholds corresponding to an average of 1 extreme event per year (λ=1), 2 events (λ=2), and 3 events (λ=3) were tested. Spatial variability 100-yr TWL variability (a). Anderson-Darling test results when adopting λ=1, λ=2, and λ=3 (b). A rejected null hypothesis indicates that the sample does not fit the exponential fit. Uncertainty of results indicating which λ leads to the highest uncertainties (c) and the lowest uncertainties (d) of return levels, based on the 95th confidence level.

3.8 Uncertainty in extreme values of TWL

Table 2 presents the overall characterization of the study area regarding TWL extremes, aggregated per EU basin, including the overall uncertainties of 100-yr TWL and its corresponding FA. Results from the sensitivity analysis on the wave contribution were not considered in the quantification of uncertainties shown as the inclusion of infragravity waves and runup would overemphasize the role of waves in TWL estimates. When looking at the entire study area, 100-yr TWL has an uncertainty of 14.5%. As more detail is added to the analysis, the 100-yr TWL uncertainty decreases to 9.2% along the Atlantic coast and 11% in the Baltic Sea, while it increases to 23% in the Mediterranean Sea. In most cases, 100-yr TWL uncertainty increases with increasing relative contribution of wave setup. Notably, the European basins with the highest relative contributions of wave setup, Central Mediterranean and Ionian Sea, are also the ones with the highest uncertainties of the 100-yr TWL. Meanwhile, in the Baltic Sea, the lower relative contribution that wave setup has on TWL could be the reason for the decrease in uncertainty.

https://doi.org/10.5194/egusphere-2025-2998
Preprint. Discussion started: 18 July 2025

Regarding the 100-yr FA, the study area presents an uncertainty of 2.5% which increases to 3.0% along the Atlantic and Mediterranean coasts and decreases to 1.7% in the Baltic Sea. However, this does not mean that the European scale map is more reliable but perhaps that it is masking some key responses coastal impacts might have when a different wave setup component is adopted. The higher uncertainties in FA are found in basins with higher magnitudes of TWL along the Atlantic coast. Oppositely, the lowest uncertainties in FA tend to occur in the Baltic Sea, where TWL magnitudes are smaller. This could be a consequence of the static flood model which is sensitive to the water level used as input, so even a slight increase in the 100-yr TWL might lead to a greater increase in FA. Overall, uncertainties in 100-yr TWL and FA do not necessarily correlate. The results show that large uncertainties in 100-yr TWL, when occurring in areas where TWL is typically low, may lead to minimal variability in FA. This is because the variations in 100-yr TWL remain small compared to changes in terrain elevation, limiting their impact on flood extent.

Table 2: Characterization of the study area based on TWL extremes and aggregated per EU basin. EVA results are summarized in TWL threshold corresponding to a λ=2 and 100-yr TWL (mean ± standard deviation). Relative contributions refer to average per basin and considering all peaks identified by POT. Uncertainties consider only tests performed in the sensitivity analyses of wave setup components and POT threshold.

EU basin	EVA		Relative contribution			Uncertainties	
	TWL threshold (m)	100-yr TWL (m)	Tide (%)	Storm surge (%)	Wave setup (%)	100-yr TWL (%)	100-yr FA (%)
Norway Sea	1.7 ± 0.3	2.4 ± 0.4	55.7	31.8	12.5	11.6	3.1
NE Atlantic	3.1 ± 1.1	3.9 ± 1.2	71.1	20.8	8.2	8.5	5.1
North Sea	2.5 ± 1.0	3.5 ± 1.1	50.1	42.4	7.5	7.0	1.8
English Channel	4.4 ± 1.5	5.1 ± 1.6	88.0	7.7	4.3	4.9	4.1
Iberia and Biscay	2.5 ± 0.5	3.0 ± 0.6	84.1	4.8	11.1	8.9	7.0
Macaronesia	1.6 ± 0.1	1.8 ± 0.2	81.3	1.2	17.5	9.4	2.1
Kattegat Bay	0.9 ± 0.1	1.7 ± 0.2	7.3	87.1	5.6	7.7	1.1
Central Baltic	0.7 ± 0.1	1.4 ± 0.3	0.6	88.1	11.3	14.3	2.3
Gulfs	0.8 ± 0.1	1.7 ± 0.3	0.3	91.7	8.0	10.5	1.1
Central Mediterranean	0.5 ± 0.1	0.7 ± 0.1	22.6	55.6	21.8	26.2	5.4
Ionian Sea	0.4 ± 0.1	0.7 ± 0.1	14.5	64.1	21.4	25.1	1.3
Adriatic Sea	0.6 ± 0.1	1.1 ± 0.2	24.4	66.1	9.5	13.8	2.3

3.9 Classification of extreme TWL events

Figure 10 presents the European classification of extreme TWL events, considering the 100-yr TWL and the dominance of TWL components regarding their relative contributions. The results show that there are no regions where the wave setup

https://doi.org/10.5194/egusphere-2025-2998
Preprint. Discussion started: 18 July 2025

dominates, although it could be an important source of extreme events, as previously shown. The highest 100-yr TWLs are found in areas where the astronomical tide dominates, mainly along the Atlantic coast. In the Baltic Sea, storm surge dominates all CTPs analyzed and the most sheltered areas are where the 100-yr TWL are the highest. In the Mediterranean Sea, the most exposed regions are where extreme events are mostly mixed, probably an indicative of the wave setup contribution which might not be enough to dominate but still relevant in decreasing the influence of the other TWL components.

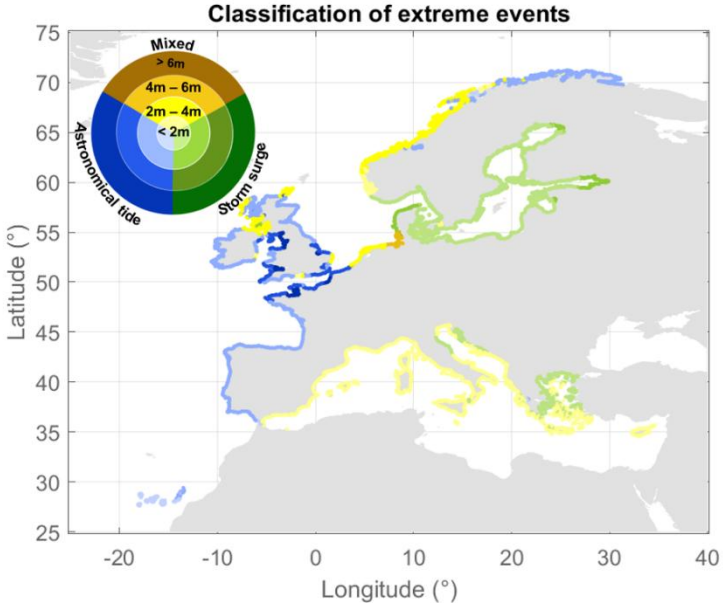

Figure 10: European classification of extreme events considering the range of 100-yr TWL and the dominance of TWL components regarding their relative contributions.

4 Discussion

Currently, there remains a strong need to provide coastal flooding maps at large geographic scales. TWL is the primary input for coastal flood modeling and must be characterized appropriately for the scale of analysis. Without a proper assessment of TWL, estimating extreme conditions becomes more uncertain (Rohmer et al., 2021; Toimil et al., 2020). However, TWL calculation is complex and presents several challenges. We have presented a methodology for estimating large-scale TWL extremes and applied it to the European coast at the highest resolution to date. For the first time, this was done using nearshore wave conditions, particularly important for semi-enclosed European seas, where offshore data can lead to TWL overestimation. The methodology incorporates spatial variability typical of large-scale coastal studies. This was achieved by using spatially and temporally variable foreshore slopes during TWL reconstruction and by applying spatially variable threshold in the POT method. An analysis of relative contributions helped the interpretation of extreme TWL behavior along the European coastline. The characterization of three macro-regions (Atlantic coast, Baltic Sea, and Mediterranean Sea)

https://doi.org/10.5194/egusphere-2025-2998
Preprint. Discussion started: 18 July 2025

supported the understanding of the degrees of uncertainty observed across different regions in distinct steps of the methodology.

One key outcome is how impactful methodological choices for wave contribution in TWL reconstruction can be. The proportion of the European floodplain which is inundated under various TWL approaches varies by up to 10%, depending on wave dataset selection, foreshore slope approach, and wave setup formulation. This area is roughly the size of the Cantabrian region in Spain or twice the size of Zeeland in the Netherlands. The most significant variation in flooded area in Europe under 100-yr TWL scenario results from changes in wave setup formulation. Using the Guza & Thornton (1981) method yields 4 – 7% more flooded area than the Stockdon et al. (2006) formulation, regardless of the foreshore slope assumption. Whereas using a constant foreshore slope yields 1% more flooded area than incorporating variable slopes. Similarly, nearshore TWL produces 3% more flooded area than offshore TWL. While these effects merit further analysis at a higher resolution and on a smaller scale, the results suggest that relying on offshore wave conditions, common in the literature, may lead to an underestimation of the actual flooded area.

A second outcome is the application of an EVA methodology appropriate for large-scale studies. The POT approach focuses on high-magnitude events, unlike annual maxima (AM) methods, that assume a single extreme event to occur per year. Our findings show that the threshold selection greatly influences sample size, particularly when applying a constant percentile threshold. Comparing our thresholds to those used in previous studies, we found that 87% of the study uses a threshold above P97 (Le Gal et al., 2023), 86.1% above P98 (Kirezci et al., 2020), and 85.8% above P98.5 (Paprotny et al., 2016). Although high, these percentages imply that a large portion of the coast would not be adequately represented using these thresholds, leading to inconsistent analysis. To ensure robust EVA approach, besides the sensitivity analysis on the threshold adopted, we also conducted an analysis on distribution fits to estimate return levels. Around 13% of the coast exhibited a significant shape parameter, justifying the use of Generalized Pareto Distribution (GPD) instead of an exponential distribution (see Supplementary Fig. S8). Most of these points presented a negative shape parameter and half of them were located in tide-dominated areas, where the TWL is modulated by the astronomical tide. However, due to the narrow confidence bands in these regions, we opted to retain the exponential fit, simplifying the method for continental-scale applications.

A third key insight is the importance of understanding the sources of extreme TWL events. Dominant TWL components provide insight into storm behaviors and potential impacts. The spatial patterns we observed had been reported before. The more exposed, tide-dominated Atlantic coast and the more sheltered and storm surge-dominated Baltic and Mediterranean Seas were identified by previous studies, even neglecting waves (Merrifield et al., 2013). However, our results differ from others in the literature due to our wave setup characterization. For example, a wave setup formulation specific to dissipative beaches, which tends to overestimate wave setup, has been adopted by other authors (Vitousek et al., 2017). This led them to understate storm surge contribution in extreme TWL in Europe, contrary to our findings. Additionally, their 111 km resolution excluded marginal seas, where we observed significant storm surge contributions. Similar patterns of storm surge contributions were identified in the Baltic Sea and of wave setup dominance in the Mediterranean Sea. Yet, lower tidal

https://doi.org/10.5194/egusphere-2025-2998
Preprint. Discussion started: 18 July 2025

contributions than what we encountered for the Atlantic coast have been reported, likely due to the inclusion of the swash component, which decreases tide influence (Melet et al., 2018). In our study, we excluded swash by using the static wave setup, as swash operates on a scale of seconds to minutes, whereas flood events typically last hours to days (Hinkel et al., 2021; Parker et al., 2023).

Finally, we highlight the importance of considering TWL as a combination of its three components. For example, as we move towards more extreme return levels, the relative contribution of storm surge increases, exposing the coast to prolonged high TWL, which can also heighten wave setup processes (Su et al., 2024). However, we acknowledge that wave setup alone cannot drive coastal flooding. On the one hand, wave setup represents an increase in mean sea level of only a few centimeters to a couple of meters (Idier et al., 2019). On the other hand, the width of the coast affected by this increase in mean sea level is only tens to a couple hundred meters long (Dodet et al., 2019). The volume of water being propagated towards the coast potentially leading to coastal flooding is not large when compared to tides and storm surges, which increase mean sea level over several kilometers of extension (Woodworth et al., 2019). Additionally, although our study shows that astronomical tide modulates extreme TWL in many regions, it should be pointed out that the main drivers of TWL driving coastal flooding are the unexpected extreme sea levels due to waves or storm surges as a result of storm conditions. This is because in physical-terms, this is an expected oscillation to which coastal communities are well adjusted to. However, our analysis shows that without the inclusion of astronomical tide, coastal flooding would probably not occur in many regions of the study area.

The methodology developed addresses the key challenges introduced regarding the TWL reconstruction and the EVA method selected. As a consequence, it also introduces new sources of uncertainties given the limitations inherited by some of the approaches adopted. For instance, even though the use of static wave setup as a component of TWL was validated, we acknowledge the possible overestimation of this component in areas such as the Baltic and Mediterranean Seas. Several factors could contribute to this. First, the use a semi-empirical setup formulation developed for open-coasts and beaches. It should be noted that although both our results and the literature indicate semi-empirical formulations as more adequate, they also present limitations (Dodet et al., 2019). For example, the formulation adopted here was not designed for use in all types of wave regimes or beach profiles (Plant & Stockdon, 2015). Second, the use of modeled foreshore slopes including capping and normalization, which may inaccurately represent the range and distributions of observed beach slopes in different coastal environments. This simplification can lead to the underestimation of the wave contribution in steep slopes or overestimation in gentler ones (Melet et al., 2020). Third, the adoption of a constant sediment grain size in the application of the Sunamura (1984) foreshore slope approximation is generic and cannot represent the entire study area. This decision might overestimate the resulting foreshore slopes in areas such as wetlands and mudflats which have finer sediment grain sizes. However, although beach types and sediment materials are diverse across the European continent, the value adopted here follow the global study by Rueda et al. (2017) and agrees with values observed in smaller scale studies across the study area (Anthony & Héquette, 2007; Duo et al., 2020; Horn & Walton, 2007).

https://doi.org/10.5194/egusphere-2025-2998
Preprint. Discussion started: 18 July 2025

Extreme TWL events can cause severe coastal impacts as water overtops land defenses, reaching communities, infrastructure, assets, and buildings (Vousdoukas et al., 2018). Proper reconstruction of TWL and its extreme events is the first step for accurate flood hazard assessment. Large-scale evaluations help us identify hotspots for more detailed risk assessments. Two key limitations of large-scale studies remain. First, the computational demands of working with large datasets are high. However, improvements in data availability and computational efficiency have enabled this study to deliver high-resolution, high-quality TWL extreme estimates across Europe. Second, simplifications and assumptions are often required to handle diverse coastal environments. In this study, the TWL as a linear sum of its components overlooks non-linear interactions between TWL components, important in regions with wide continental shelves and enclosed lagoons (Bertin et al., 2012; Lorenz et al., 2023), such as the Baltic and Mediterranean Seas. According to Arns et al. (2020), by not considering non-linear interactions between tide and storm surge, for example, can lead to 30% increase in estimated extreme water levels, 16% increase in coastal flooding costs, and 8% increase in exposed people globally. A strategy to address such issue at the large-scale is to run a hydrodynamic model with both tidal and meteorological forcings combined (Haigh et al., 2014b). This approach, however, does not consider the contribution of waves.

Finally, we point out that although this study present extreme TWL at an unprecedented resolution for the entire coastal zone of Europe, one could find diversifications of beach profiles and types, from sandy to rocky formations, within the 1 km distance adopted. Thus, although the TWL resolution adopted here is unprecedented at this scale, it remains insufficient for local-scale applications, where higher-resolution data are needed to support detailed planning.

Data availability

The data generated in this study have been deposited in the Zenodo database under accession code 10.5281/zenodo.15111961.

Author contributions

Conceptualization: AT, IJL. Methodology: AT, IJL, MM, HL. Formal analysis: CC. Validation: CC, AT, MM, HL. Writing – original draft: CC. Writing – review and editing: AT, IJL, MM, HL. Project administration: AT, MM. Funding acquisition: AT, IJL.

Acknowledgements

This study was funded by the grant COASTALfutures (PID2021-126506OB-100); the Government of Cantabria trough the FENIX Project; and the European Union's Horizon 2020 CoCliCo Project (grant agreement No 101003598). CC

https://doi.org/10.5194/egusphere-2025-2998
Preprint. Discussion started: 18 July 2025

acknowledges the financial support of the Concepción Arenal Fellowship 2021 of the Universidad de Cantabria (UC-21-19). AT was economically supported by the Spanish Government through the Ramon y Cajal Programme (RYC2021-030873-I).

References

Anthony, E. J., & Héquette, A. (2007). The grain-size characterisation of coastal sand from the Somme estuary to Belgium: Sediment sorting processes and mixing in a tide- and storm-dominated setting. *Sedimentary Geology*, *202*(3), 369–382. https://doi.org/10.1016/j.sedgeo.2007.03.022

Arns, A., Wahl, T., Haigh, I. D., Jensen, J., & Pattiaratchi, C. (2013). Estimating extreme water level probabilities: A comparison of the direct methods and recommendations for best practise. *Coastal Engineering*, *81*, 51–66. https://doi.org/10.1016/j.coastaleng.2013.07.003

Arns, A., Wahl, T., Wolff, C., Vafeidis, A. T., Haigh, I. D., Woodworth, P., Niehüser, S., & Jensen, J. (2020). Non-linear interaction modulates global extreme sea levels, coastal flood exposure, and impacts. *Nature Communications*, *11*(1), 1–9. https://doi.org/10.1038/s41467-020-15752-5

Barboza, F. R., & Defeo, O. (2015). Global diversity patterns in sandy beach macrofauna: A biogeographic analysis. *Scientific Reports*, *5*, 1–9. https://doi.org/10.1038/srep14515

Barnard, P. L., Erikson, L. H., Foxgrover, A. C., Hart, J. A. F., Limber, P., O'Neill, A. C., van Ormondt, M., Vitousek, S., Wood, N., Hayden, M. K., & Jones, J. M. (2019). Dynamic flood modeling essential to assess the coastal impacts of climate change. *Scientific Reports*, *9*(1), 1–13. https://doi.org/10.1038/s41598-019-40742-z

Bertin, X., Bruneau, N., Breilh, J. F., Fortunato, A. B., & Karpytchev, M. (2012). Importance of wave age and resonance in storm surges: The case Xynthia, Bay of Biscay. *Ocean Modelling*, *42*, 16–30. https://doi.org/10.1016/j.ocemod.2011.11.001

Bezak, N., Brilly, M., & Šraj, M. (2014). Comparaison entre les méthodes de dépassement de seuil et du maximum annuel pour les analyses de fréquence des crues. *Hydrological Sciences Journal*, *59*(5), 959–977. https://doi.org/10.1080/02626667.2013.831174

Cabrita, P., Montes, J., Duo, E., Brunetta, R., & Ciavola, P. (2024). The Role of Different Total Water Level Definitions in Coastal Flood Modelling on a Low-Elevation Dune System. *Journal of Marine Science and Engineering*, *12*(6), 1003. https://doi.org/10.3390/jmse12061003

Camus, P., Mendez, F. J., Medina, R., & Cofiño, A. S. (2011). Analysis of clustering and selection algorithms for the study of multivariate wave climate. *Coastal Engineering*, *58*(6), 453–462. https://doi.org/10.1016/j.coastaleng.2011.02.003

Camus, P., Mendez, F. J., Medina, R., Tomas, A., & Izaguirre, C. (2013). High resolution downscaled ocean waves (DOW) reanalysis in coastal areas. *Coastal Engineering*, *72*, 56–68. https://doi.org/10.1016/j.coastaleng.2012.09.002

Coles, S. (2001). *An Introduction to Statistical Modeling of Extreme Values*. Springer series in statistics: London (UK).

Copernicus. (2019). *DEM - Global and European Digital Elevation Model*. https://dataspace.copernicus.eu/explore-data/data-collections/copernicus-contributing-missions/collections-description/COP-DEM

Dodet, G., Melet, A., Ardhuin, F., Bertin, X., Idier, D., & Almar, R. (2019). The Contribution of Wind-Generated Waves to Coastal Sea-Level Changes. *Surveys in Geophysics* (Vol. 40, Issue 6). Springer Netherlands. https://doi.org/10.1007/s10712-019-09557-5

Duo, E., Sanuy, M., Jiménez, J. A., & Ciavola, P. (2020). How good are symmetric triangular synthetic storms to represent real events for coastal hazard modelling. *Coastal Engineering*, *159*(May). https://doi.org/10.1016/j.coastaleng.2020.103728

https://doi.org/10.5194/egusphere-2025-2998
Preprint. Discussion started: 18 July 2025

Egbert, G. D., & Erofeeva, S. Y. (2002). Efficient inverse modeling of barotropic ocean tides. *Journal of Atmospheric and Oceanic Technology*, *19*(2), 183–204. https://doi.org/10.1175/1520-0426(2002)019<0183:EIMOBO>2.0.CO;2

Gomes da Silva, P., Coco, G., Garnier, R., & Klein, A. H. F. (2020). On the prediction of runup, setup and swash on beaches. *Earth-Science Reviews*, *204*(March), 103148. https://doi.org/10.1016/j.earscirev.2020.103148

Guza, R. T., & Thornton, E. B. (1981). Wave set-up on a natural beach. *Journal of Geophysical Research*, *86*(C5), 4133–4137. https://doi.org/10.1029/JC086iC05p04133

Haigh, I. D., MacPherson, L. R., Mason, M. S., Wijeratne, E. M. S., Pattiaratchi, C. B., Crompton, R. P., & George, S. (2014a). Estimating present day extreme water level exceedance probabilities around the coastline of Australia: Tropical cyclone-induced storm surges. *Climate Dynamics*, *42*(1–2), 139–157. https://doi.org/10.1007/s00382-012-1653-0

Haigh, I. D., Wijeratne, E. M. S., MacPherson, L. R., Pattiaratchi, C. B., Mason, M. S., Crompton, R. P., & George, S. (2014b). Estimating present day extreme water level exceedance probabilities around the coastline of Australia: Tides, extra-tropical storm surges and mean sea level. *Climate Dynamics*, *42*(1–2), 121–138. https://doi.org/10.1007/s00382-012-1652-1

Harley, M. (2017). Coastal Storm Definition. In: Ciavola, P., Coco, G., (Ed.), *Coastal Storms: Processes and Impacts*, First Edition, Wiley Blackwell: 1 – 22. https://doi.org/10.1002/9781118937099.ch1

Hersbach, H., Bell, B., Berrisford, P., Hirahara, S., Horányi, A., Muñoz-Sabater, J., Nicolas, J., Peubey, C., Radu, R., Schepers, D., Simmons, A., Soci, C., Abdalla, S., Abellan, X., Balsamo, G., Bechtold, P., Biavati, G., Bidlot, J., Bonavita, M., De Chiara, G., Dahlgren, P., Dee, D., Diamantakis, M., Dragani, R., Flemming, J., Forbes, R., Fuentes, M., Geer, A., Haimberger, L., Healy, S., Hogan, R.J., Hólm, E., Janisková, M., Keeley, S., Laloyaux, P., Lopez, P., Lupu, C., Radnoti, G., de Rosnay, P., Rozum, I., Vamborg, F., Villaume, S., Thépaut, J. N. (2020). The ERA5 global reanalysis. *Quarterly Journal of the Royal Meteorological Society*, *146*(730), 1999–2049. https://doi.org/10.1002/qj.3803

Hinkel, J., Feyen, L., Hemer, M., Le Cozannet, G., Lincke, D., Marcos, M., Mentaschi, L., Merkens, J. L., de Moel, H., Muis, S., Nicholls, R. J., Vafeidis, A. T., van de Wal, R. S. W., Vousdoukas, M. I., Wahl, T., Ward, P. J., & Wolff, C. (2021). Uncertainty and Bias in Global to Regional Scale Assessments of Current and Future Coastal Flood Risk. *Earth's Future*, *9*(7), 1–28. https://doi.org/10.1029/2020EF001882

Horn, D. P., & Walton, S. M. (2007). Spatial and temporal variations of sediment size on a mixed sand and gravel beach. *Sedimentary Geology*, *202*(3), 509–528. https://doi.org/10.1016/j.sedgeo.2007.03.023

Idier, D., Bertin, X., Thompson, P., & Pickering, M. D. (2019). Interactions Between Mean Sea Level, Tide, Surge, Waves and Flooding: Mechanisms and Contributions to Sea Level Variations at the Coast. *Surveys in Geophysics*, *40*(6), 1603–1630. https://doi.org/10.1007/s10712-019-09549-5

Kirezci, E., Young, I. R., Ranasinghe, R., Muis, S., Nicholls, R. J., Lincke, D., & Hinkel, J. (2020). Projections of global-scale extreme sea levels and resulting episodic coastal flooding over the 21st Century. *Scientific Reports*, *10*(1), 1–12. https://doi.org/10.1038/s41598-020-67736-6

Le Gal, M., Fernández-Montblanc, T., Duo, E., Montes Perez, J., Cabrita, P., Souto Ceccon, P., Gastal, V., Ciavola, P., & Armaroli, C. (2023). A new European coastal flood database for low-medium intensity events. *Natural Hazards and Earth System Sciences*, *23*(11), 3585–3602. https://doi.org/10.5194/nhess-23-3585-2023

Liu, H., Yang, F., & Wang, H. (2023). Research on Threshold Selection Method in Wave Extreme Value Analysis. *Water (Switzerland)*, *15*(20). https://doi.org/10.3390/w15203648

Lobeto, H., Semedo, A., Lemos, G., Dastgheib, A., Menendez, M., Ranasinghe, R., & Bidlot, J.-R. (2024). Global coastal wave storminess. *Scientific Reports*, *14*(1). https://doi.org/10.1038/s41598-024-51420-0

Lorenz, M., Arns, A., & Gräwe, U. (2023). How Sea Level Rise May Hit You Through the Backdoor: Changing Extreme

https://doi.org/10.5194/egusphere-2025-2998
Preprint. Discussion started: 18 July 2025

Water Levels in Shallow Coastal Lagoons. *Geophysical Research Letters*, *50*(21), 1–11. https://doi.org/10.1029/2023GL105512

Melet, A., Almar, R., Hemer, M., Le Cozannet, G., Meyssignac, B., & Ruggiero, P. (2020). Contribution of Wave Setup to Projected Coastal Sea Level Changes. *Journal of Geophysical Research: Oceans*, *125*(8). https://doi.org/10.1029/2020JC016078

Melet, A., Meyssignac, B., Almar, R., & Le Cozannet, G. (2018). Under-estimated wave contribution to coastal sea-level rise. *Nature Climate Change*, *8*(3), 234–239. https://doi.org/10.1038/s41558-018-0088-y

Merrifield, M. A., Genz, A. S., Kontoes, C. P., & Marra, J. J. (2013). Annual maximum water levels from tide gauges: Contributing factors and geographic patterns. *Journal of Geophysical Research: Oceans*, *118*(5), 2535–2546. https://doi.org/10.1002/jgrc.20173

Muis, S., Verlaan, M., Winsemius, H., Aerts, J., & Ward, P. (2015). The first global-scale hidncast of extreme sea levels. *E-Proceedings of the 36th IAHR World Congress*, *1*, 6177–6182.

Muis, S., Verlaan, M., Winsemius, H. C., Aerts, J. C. J. H., & Ward, P. J. (2016). A global reanalysis of storm surges and extreme sea levels. *Nature Communications*, *7*(May). https://doi.org/10.1038/ncomms11969

Neumann, B., Vafeidis, A. T., Zimmermann, J., & Nicholls, R. J. (2015). Future Coastal Population Growth and Exposure to Sea-Level Rise and Coastal Flooding - A Global Assessment. *PLoS ONE*, *10*(3), 1–34.

Paprotny, D., Morales-Nápoles, O., & Nikulin, G. (2016). Extreme sea levels under present and future climate: A pan-European database. *E3S Web of Conferences*, *7*. https://doi.org/10.1051/e3sconf/20160702001

Paprotny, D., Morales-Nápoles, O., Vousdoukas, M. I., Jonkman, S. N., & Nikulin, G. (2018). Accuracy of pan-European coastal flood mapping. *Journal of Flood Risk Management*, *12*(2), 1–16. https://doi.org/10.1111/jfr3.12459

Parker, K., Erikson, L., Thomas, J., Nederhoff, K., Barnard, P., & Muis, S. (2023). Relative contributions of water-level components to extreme water levels along the US Southeast Atlantic Coast from a regional-scale water-level hindcast. *Natural Hazards*, *117*(3), 2219–2248. https://doi.org/10.1007/s11069-023-05939-6

Plant, N. G., & Stockdon, H. F. (2015). How well can wave runup be predicted? Comment on Laudier et al. (2011) and Stockdon et al. (2006). *Coastal Engineering*, *102*, 44–48. https://doi.org/10.1016/j.coastaleng.2015.05.001

Pugh, D. (1987). *Tides, surges and mean sea level* A Handbook for Engineers and Scientists. Wiley, Chichester, p. 472.

Pugh, D., & Woodworth, P. (2014). *Sea-Level Science: Understanding Tides, Surges, Tsunamis and Mean Sea-Level Changes* (2nd ed.). Cambridge University Press.

Rashid, M. M., Wahl, T., & Chambers, D. P. (2021). Extreme sea level variability dominates coastal flood risk changes at decadal time scales. *Environmental Research Letters*, *16*(2). https://doi.org/10.1088/1748-9326/abd4aa

Rasmussen, D. J., Kulp, S., Kopp, R. E., Oppenheimer, M., & Strauss, B. H. (2022). Popular extreme sea level metrics can better communicate impacts. *Climatic Change*, *170*(3–4). https://doi.org/10.1007/s10584-021-03288-6

Rohmer, J., Lincke, D., Hinkel, J., Le Cozannet, G., Lambert, E., & Vafeidis, A. T. (2021). Unravelling the importance of uncertainties in global-scale coastal flood risk assessments under sea level rise. *Water (Switzerland)*, *13*(6), 1–18. https://doi.org/10.3390/w13060774

Rueda, A., Vitousek, S., Camus, P., Tomas, A., Espejo, A., Losada, I. J., Barnard, P. L., Erikson, L. H., Ruggiero, P., Reguero, B. G., & Mendez, F. J. (2017). A global classification of coastal flood hazard climates associated with large-scale oceanographic forcing. *Scientific Reports*, *7*, 5038. 10.1038/s41598-017-05090-w

Serafin, K. A., Ruggiero, P., Barnard, P. L., & Stockdon, H. F. (2019). The influence of shelf bathymetry and beach topography on extreme total water levels: Linking large-scale changes of the wave climate to local coastal hazards. *Coastal Engineering*, *150*(January), 1–17. https://doi.org/10.1016/j.coastaleng.2019.03.012

https://doi.org/10.5194/egusphere-2025-2998
Preprint. Discussion started: 18 July 2025

Shchepetkin, A. F., & McWilliams, J. C. (2005). The regional oceanic modeling system (ROMS): A split-explicit, free-surface, topography-following-coordinate oceanic model. *Ocean Modelling*, *9*(4), 347–404. https://doi.org/10.1016/j.ocemod.2004.08.002

Soomere, T., Eelsalu, M., & Pindsoo, K. (2018). Variations in parameters of extreme value distributions of water level along the eastern Baltic Sea coast. *Estuarine, Coastal and Shelf Science*, *215*(October), 59–68. https://doi.org/10.1016/j.ecss.2018.10.010

Stockdon, H. F., Holman, R. A., Howd, P. A., & Sallenger, A. H. (2006). Empirical parameterization of setup , swash , and runup. *Coastal Engineering 53*, 573–588. https://doi.org/10.1016/j.coastaleng.2005.12.005

Su, J., Murawski, J., Nielsen, J. W., & Madsen, K. S. (2024). Coinciding storm surge and wave setup: A regional assessment of sea level rise impact. *Ocean Engineering*, *305*(January). https://doi.org/10.1016/j.oceaneng.2024.117885

Sunamura, T. (1984). Quantitative Predictions of Beach-Face Slopes. *Bulletin of the Geological Society of America*, *95*(2), 242–245. https://doi.org/10.1130/0016-7606(1984)95<242:qpobs>2.0.co;2

Toimil, A., Losada, I. J., Nicholls, R. J., Dalrymple, R. A., & Stive, M. J. F. (2020). Addressing the challenges of climate change risks and adaptation in coastal areas: A review. *Coastal Engineering*, *156*(July 2019). https://doi.org/10.1016/j.coastaleng.2019.103611

Tolman, H. L. (2009). User manual and system documentation of WAVEWATCH-IIITM version 3.14. *Technical Note*, *3.14*, 220.

USACE, US Army Corps of Engineers. (1984). Shore Protection Manual. In *US Government Printing Office* (4th ed., Vol. 1). (U.S. Govt, Washington, D.C., 1984)

Vafeidis, A. T., Nicholls, R. J., McFadden, L., Tol, R. S. J., Hinkel, J., Spencer, T., Grashoff, P. S., Boot, G., & Klein, R. J. T. (2008). A new global coastal database for impact and vulnerability analysis to sea-level rise. *Journal of Coastal Research*, *24*(4), 917–924. https://doi.org/10.2112/06-0725.1

Vitousek, S., Barnard, P. L., Fletcher, C. H., Frazer, N., Erikson, L., & Storlazzi, C. D. (2017). Doubling of coastal flooding frequency within decades due to sea-level rise. *Scientific Reports*, *7*(1), 1–9. https://doi.org/10.1038/s41598-017-01362-7

Vousdoukas, M. I., Bouziotas, D., Giardino, A., Bouwer, L. M., Mentaschi, L., Voukouvalas, E., & Feyen, L. (2018). Understanding epistemic uncertainty in large-scale coastal flood risk assessment for present and future climates. *Natural Hazards and Earth System Sciences*, *18*(8), 2127–2142. https://doi.org/10.5194/nhess-18-2127-2018

Vousdoukas, M. I., Voukouvalas, E., Mentaschi, L., Dottori, F., Giardino, A., Bouziotas, D., Bianchi, A., Salamon, P., & Feyen, L. (2016). Developments in large-scale coastal flood hazard mapping. *Natural Hazards and Earth System Sciences*, *16*(8), 1841–1853. https://doi.org/10.5194/nhess-16-1841-2016

Wang, P., & Bernier, N. B. (2023). Adding sea ice effects to a global operational model (NEMO v3.6) for forecasting total water level: Approach and impact. *Geoscientific Model Development*, *16*(11), 3335–3354. https://doi.org/10.5194/gmd-16-3335-2023

Woodworth, P. L., Melet, A., Marcos, M., Ray, R. D., Wöppelmann, G., Sasaki, Y. N., Cirano, M., Hibbert, A., Huthnance, J. M., Monserrat, S., & Merrifield, M. A. (2019). Forcing Factors Affecting Sea Level Changes at the Coast. *Surveys in Geophysics* (Vol. 40, Issue 6). Springer Netherlands. https://doi.org/10.1007/s10712-019-09531-1